

First-principles calculations of the structure of MgSiO₃ melt at high temperature and high pressure

MATSUI, Masanori^{1*}

¹School of Sci., Univ. of Hyogo

Crystals and melts with MgSiO₃ composition are important constituents of the Earth's lower crust and mantle. Therefore an accurate knowledge of their structural and elastic properties at high temperatures and high pressures is crucial to investigate the chemical and physical structures, and the conditions of formation and evolution of the Earth. However, reliable experimental data under geophysically relevant conditions are generally lacking for MgSiO₃ melt, mainly due to the difficulty in obtaining such data at the combined high temperature and high pressure found in the Earth's interior. Here we use the first-principles molecular dynamics (FPMD) method to study the structures and elastic properties of MgSiO₃ melt at high temperatures and high pressures.

All calculations were performed with the Vienna Ab Initio Simulation Package VASP (Kresse and Furthmuller, 1996). The projector-augmented wave (PAW) method was used in the local density approximation (LDA) for the exchange-correlation functional (Blochl, 1994; Kresse and Joubert, 1999). FPMD calculations were carried out in the canonical ensemble (constant temperature T , constant volume V , and constant number of atoms N in the system) using cubic basic cells. N was taken to be 160 (32 MgSiO₃) throughout this study. After annealing the system sufficiently at 4000 K, and then 3000 K, we fixed V at 38.54 cm³/mol and T at 2000 K to calculate the interference function $S(Q)$, where Q is the length of scattering vector, and the radial distribution function (RDF) for each atom pair. We found FPMD calculated $S(Q)$ compares reasonably well with the observed data from X-ray analyses at 1973 K by Waseda and Toguri(1990). The FPMD predicted average nearest neighbor bond distances $r(ij)$, and coordination numbers $n(ij)$ between atoms i and j are also compared well with the data by Waseda and Toguri(1990), except the $r(\text{MgO})$ distance, in which the FPMD value of 1.97 Å is much shorter than the value [2.12(1) Å] by the X-ray analyses. We further apply the FPMD technique to investigate the temperature and pressure dependencies of the structure of MgSiO₃ melt.

Keywords: MgSiO₃ melt, high temperature, high pressure, first-principles calculation

Forsterite-MgSiO₃ liquid interface : molecular dynamics perspective

NORITAKE, Fumiya^{1*} ; KAWAMURA, Katsuyuki¹

¹Okayama University

Knowledge about the viscosity and permeability of partial molten rocks is important to understand the thermal history of the Earth and volcanisms. For understanding those obtained by experiments and estimating the physical properties at extreme conditions those are difficult to reproduce in laboratory experiments, the knowledge about structure and properties of silicate crystal-liquid interfaces is necessary. The properties of melt as sandwiched thin films are considered as being different with ones in bulk melts by the effect of crystal surface. For instance, lateral self-diffusivity of water to crystal surfaces shows different from bulk one in the case of water-brucite surface (Sakuma et al. 2003), water-muscovite mica surface (Sakuma and Kawamura, 2009). The dynamic property anomalies on solid - liquid surfaces affect properties of bulk rock such as permeability (Ichikawa et al. 2001).

In this study, structure and properties of the forsterite-MgSiO₃ liquid interfaces are investigated by using molecular dynamics simulations. It is essential to know the structure and physical properties of forsterite-MgSiO₃ liquid interfaces since forsterite is the liquidus mineral of primordial magmas.

Molecular dynamics simulations were performed with NPT ensemble using MXDORTO code (Sakuma and Kawamura, 2009). The initial structure is a 21440 atom system in which a sheet of MgSiO₃ liquid consist of 8000 atoms (~5 nm) is sandwiched between (010) surfaces of forsterite(Pbnm) and 43440 atom system in which a sheet of MgSiO₃ liquid consist of 30000 atoms (~20 nm) is sandwiched between (010) surfaces of forsterite. Firstly we calculated equilibrated MgSiO₃ liquid film in vacuum starting with a randomly generated structure and randomly generated velocities of atoms through 0.5 ns (1,000,000 steps) at 1973 K and quench to 300 K. Secondly we calculated a bulk forsterite crystal with 13440 atoms (11*5*8 unit cells of forsterite(Pbnm)) starting with a given experimental crystal structure which was obtained by the experiment [5] and with randomly generated velocities of atoms and then cut along (010) surface. Finally we combined forsterite cut along (010) surface and MgSiO₃ liquid film. Under maintaining isobaric and isothermal conditions, we performed the relaxation of 0.5~1.5 ns. Then the statistical averages of the structure and physical properties were obtained from the velocities and coordinates of each atom in the simulations through 500 ps. The function of inter-atomic potential model was same as used in our previous work (Noritake et al. 2012).

By these simulations, characteristic structures in the forsterite-MgSiO₃ liquid interface are observed. The layered structure of alternated crystal surface, Si-rich and Mg-rich layers in the crystal-liquid interface was observed. The layered structure was formed by energy difference between Si-O semi-covalent bonds and Mg-O ionic bonds. Si-O-Si bridging and free oxygen atoms are excessively formed and in the near surface since the energy of Si-O bonding is much lower than that of Mg-O bonding. The difference of layered structure by thickness of MgSiO₃ liquid film might be caused by the difference of the degree of freedom of configuration in liquid film. The two-dimensional diffusivity of oxygen atoms is controlled by two factors. The one is the thickness of liquid film that decreases oxygen diffusivity with decreasing the film thickness because of decrease of degree of freedom of configuration in liquid film. The other is composition of sliced layer where oxygen diffusivity increases with increasing the Mg/Si ratio since Si-O bonding is much stronger than Mg-O ones.

Keywords: Interface, High-Temperature, Silicates, Molecular dynamics simulation

Phase transitions in Zn_2SiO_4 : first-principles study

KANZAKI, Masami^{1*}

¹Inst. Study Earth's Interior, Okayama University

Recent experimental study (Liu et al., *PCM*, 40, 467, 2013) suggested that high-pressure phases of III and IV in Zn_2SiO_4 could be retrograde phases transformed during decompression. In order to check stabilities of these phases under pressure, and to find original high-pressure phases, density functional theory total energy calculations of 12 phases at 0 K have been conducted.

Three pressure-induced "phase transitions" during structural optimization were observed: phase II to spinel structure, phase III to a new high-pressure phase, and phase IV to Na_2SO_4 III-type structure. Phase III, having tetrahedral olivine structure, exhibited extraordinary high compressibility, which is due to large volume reductions in vacant octahedral sites corresponding M1 and M2 sites in olivine structure. Calculated enthalpies of the phases at 0 K confirmed that phase III and IV are not stable at any pressure. It also suggested that Na_2SO_4 III and II phases will be stable phases replacing phase III and IV, respectively.

Keywords: Zn_2SiO_4 , phase transition, high pressure phase, first-principles, transition mechanism

A new high pressure phase of Fe₂SiO₄ and the relationship between spin and structural transitions

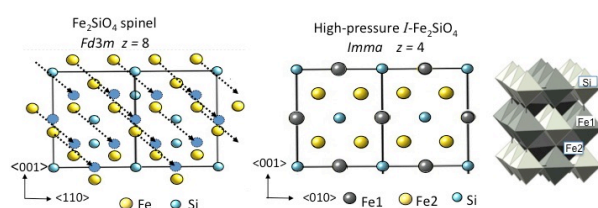
YAMANAKA, Takamitsu^{1*}; KYONO, Atsushi²; NAKAMOTO, Yuki³; KHARLAMOVA, Svetlana¹; STRUZKIN, Viktor¹; MAO, Ho-kwang¹; HEMLY, Russell¹

¹Carnegie Institution of Washington Geophysical Laboratory, ²Division of Earth Evolution Sciences, Life and Environment Sciences, University of Tsukuba, ³Center for Quantum Science and Technology Under Extreme Conditions, Osaka University

A structural change in Fe₂SiO₄ spinel (ringwoodite) has been found by synchrotron powder diffraction study and the structure of a new high-pressure phase was determined by Monte-Carlo simulation method and Rietveld profile fitting of x-ray diffraction data up to 64 GPa at ambient temperature. A transition from the cubic spinel structure to a body centered orthorhombic phase (I-Fe₂SiO₄) with space group *Imma* and Z=4 was observed at approximately 34 GPa. The structure of I-Fe₂SiO₄ has two crystallographically independent FeO₆ octahedra. Iron resides in two different sites of six-fold coordination: Fe1 and Fe2, which are arranged in layers parallel to (101) and (011), and very similar to the layers of FeO₆ octahedra in the spinel structure. Silicon is located in the six-fold coordination in I-Fe₂SiO₄. The transformation to the new high-pressure phase is reversible under decompression at ambient temperature. A martensitic transformation of each slab of the spinel structure with transition vector $\langle 1/8 \ 1/8 \ 1/8 \rangle$ generates the I-Fe₂SiO₄ structure. Laser heating of I-Fe₂SiO₄ at 1500 K results in a decomposition of the material to rhombohedral FeO and SiO₂ stishovite.

Fe K beta x-ray emission measurements at high pressure up to 65GPa show that the transition from a high spin (HS) to an intermediate spin (IS) state begins at 17 GPa in the spinel phase. The IS electron spin state is gradually enhanced with pressure. The Fe²⁺ ion at the octahedral site changes the iron radius under compression from 0.78 Å at the high-spin state to 0.61 Å at the low spin, which results in the changes of the lattice parameter and the deformation of the octahedra of the spinel structure. The compression curve of the lattice parameter of the spinel is discontinuous at approximately 20 GPa. The spin transition induces an isostructural change.

Keywords: Fe₂SiO₄ spinel, new high-pressure phase, spin transition, X-ray emission, martensitic transition



Synchrotron Mössbauer spectroscopy on Fe₃S, FeO and natural almandine

KAMADA, Seiji^{1*}; HIRAO, Naohisa²; HAMADA, Maki³; SUZUKI, Nanami¹; OHTANI, Eiji¹; OHISHI, Yasuo²; MASUDA, Ryo⁴; MITSUI, Takaya⁵

¹Tohoku Univ., ²JASRI, ³School of Nature system, College of Science and Engineering, Kanazawa University, ⁴Research Reactor Institute, Kyoto Univ., ⁵JAEA

The Earth's core is considered to be composed of an iron alloy with light elements since its density is smaller than that of pure iron under core conditions (e.g., Birch, 1964; Dubrovinsky et al., 2000). Although there are many candidates for these elements, such as H, C, O, Si, and S, sulfur in particular has been considered as one of the most plausible candidates. This is because it is depleted in the mantle, suggesting that it exists in the Earth's core (Murthy and Hall, 1970), and iron sulfides are found universally in iron meteorites, i.e., analogues of the Earth's core. Although the content of sulfur in the Earth's core is not known precisely, the sulfur content in the core is estimated to be at least a few wt% based on cosmic element abundances (McDonough, 2003) and high pressure partitioning experiments (e.g., Hillgren et al., 2000).

Since sulfur is one of the most plausible light elements, a compressibility and phase diagram in the Fe-FeS system has been studied (e.g., Campbell et al., 2007; Chen et al., 2007; Fei et al., 2000; Kamada et al., 2010; Li et al., 2001; Seagle et al., 2006). According to previous studies, Fe₃S is stable from 21 GPa and at least up to 200 GPa. Therefore, Fe₃S can be one of a candidate of the inner core materials. In addition, a synchrotron Mössbauer spectroscopy (SMS) and X-ray emission spectroscopic studies on Fe₃S revealed a spin transition and magnetic transition between 20 and 25 GPa (Lin et al., 2004; Shen et al., 2003). It also showed an abnormal evolution of a and c axes with increasing pressure (Chen et al., 2007).

Synchrotron Mössbauer spectroscopy is a good probe of a small sample under high pressure to investigate magnetic properties and electronic states of Fe of core and mantle minerals. An energy domain Mössbauer spectroscopic system has been recently developed at the BL10XU, SPring-8. We have measured Mössbauer spectra from Fe₃S and FeO under high pressure and a natural almandine at ambient pressure.

A powder mixture was made from ⁵⁷Fe (96.63%, ISOFLEX) and FeS (99.9%, RAREMETALLIC co., LTD.) with a ratio of Fe:S=75.0:25.0 (in at%). A foil was made from the mixture by a cold compression using a diamond anvil cell (DAC) and loaded into a sample chamber. ⁵⁷Fe enriched Fe₃S was synthesized from the powder mixture in a DAC at 30 GPa and 1350 K. The synthesis of Fe₃S was confirmed by X-ray diffraction patterns at BL10XU, SPring-8. ⁵⁷FeO was made by reducing from ⁵⁷Fe₂O₃ (ISOFLEX) at ambient pressure and high temperature. A pellet was made from ⁵⁷FeO powder and loaded into a sample chamber of a DAC. We also measured Mössbauer spectra of a natural almandine (Py_{15.7}Alm_{78.6}Gros_{4.4}Sp_{1.3}, Idaho, USA). The energy of used X-ray for Mössbauer spectroscopy was 14.4125 keV.

We have measured Mössbauer spectra of Fe₃S during decompression at 5, 15, 20, 25, and 30 GPa and room temperature at BL10XU and BL11XU. At BL10XU, those of FeO and the almandine were obtained at 200 GPa and ambient pressure, respectively. The magnetic transition in Fe₃S was observed between 20 and 25 GPa, which is consistent with Lin et al. (2004). We observed doublet peaks from FeO. An evidence of Fe³⁺ in the almandine was not detected in this study. We will report the results of the Mössbauer spectra based on the newly developed system at BL10XU, SPring-8.

Keywords: Earth's core, Mantle, Mössbauer, Fe₃S, FeO

Temperature dependence of Fe³⁺, Al and Ga distributions and local domain structure in synthetic Ca-clinopyroxene

AKASAKA, Masahide^{1*}; HAMADA, Maki²; NAGASHIMA, Mariko³; EJIMA, Terumi⁴

¹Dep. Geoscience, Shimane Univ., ²School of Nature system, Kanazawa Univ., ³Dept. Earth Sci., Yamaguchi Univ., ⁴AIST

Distribution of Fe³⁺, Al³⁺ and Ga³⁺ among octahedral and tetrahedral sites in synthetic esseneite (CaFeAlSiO₆)- and (CaFe³⁺GaSiO₆)₉₀(CaGa₂SiO₆)₁₀-clinopyroxenes at 800 and 1200 °C were investigated using ⁵⁷Fe Mössbauer and X-ray Rietveld methods to find a relation between site occupancies of trivalent cations at the octahedral and tetrahedral sites and ionic sizes of trivalent cations. The esseneite was synthesized from oxide mixture using sintering technique at 1200 °C in air. The FeGaTs₉₀GaTs₁₀-Cpx was crystallized from glass starting material at 1200 °C in air. The Cpxs synthesized and those annealed at 800 °C were analyzed using ⁵⁷Fe Mössbauer spectroscopic and X-ray Rietveld methods. In the synthetic esseneite, ^VFe³⁺:^{IV}Fe³⁺-ratio at 800 °C was determined as 82(1):18(1) by Mössbauer method and 78.2(5):21.8(5) by Rietveld method, whereas, at 1200 °C, 79(1):21(1) by Mössbauer method and 77(1):23(1) by Rietveld analysis. The resulting Fe³⁺ populations at octahedral M1 and tetrahedral T sites in the synthetic esseneite are Fe³⁺0.782(5)-0.82(1) apfu and 0.218(5)-0.18(1) apfu, respectively. In the synthetic Fe³⁺-Ga-Cpx, ^VFe³⁺:^{IV}Fe³⁺-ratio at 800 °C was 74(3):26(2) (Mössbauer analysis data) and 78(1):22(1) (Rietveld analysis data), while, at 1200 °C, 71(3):29(1) (Mössbauer analysis data) and 67(1):33(1) (Rietveld analysis), which results in populations at the octahedral M1 and tetrahedral T sites of [Fe³⁺_{0.67(1)-0.70(1)}Ga_{0.33-0.30}]^{M1}[Si_{1.0}Fe³⁺_{0.23-0.20}

Ga_{0.77-0.80}]^T (O = 6) at 800 °C, and [Fe³⁺_{0.64(1)-0.60(1)}Ga_{0.36-0.40}]^{M1}[Si_{1.0}Fe³⁺_{0.26-0.30}Ga_{0.74-0.70}]^T at 1200 °C. This result indicates the temperature dependence of Fe³⁺, Al³⁺ and Ga³⁺ distributions between M1 and T sites. However, it is evident that, even at different temperatures, distributions of Fe³⁺, Al³⁺ and Ga³⁺ between M1 and T sites are well correlated with the ratio of ionic radius of larger Fe³⁺-cation against smaller Al³⁺ and Ga³⁺, as Akasaka et al. (1997) indicated. Another finding in this study is the splitting of a ⁵⁷Fe Mössbauer doublet by Fe³⁺ at M1 site into two doublets. This indicates existence of short-range domain structure by two kinds of M1 sites with slightly different distortions, which cannot be detected by X-ray diffraction.

Keywords: clinopyroxene, Mossbauer analysis, X-ray structural refinement, Crystal chemistry, ionic distributions, temperature dependence

Phase Transformation of Zirconium under High P-T Conditions

ONO, Shigeaki^{1*}

¹JAMSTEC

The behavior of zirconium metal under high pressures is important in the community of the high-pressure study, because changes in resistivity due to the phase transformations of zirconium (Zr) are used as pressure calibration points in the high-pressure experiments. Zirconium metal, which shows the hcp structure at ambient conditions, is known to transform to the bcc structure (beta phase) above 1135 K at ambient pressure. With increasing pressure, phase transformations to a hexagonal structure (omega phase), at the pressure around 5 GPa and to a bcc structure around 30 GPa have been observed at room temperature. The formation of the high-pressure phases is concerned with changes in the electronic structure. Recent investigations for the phase transformation from the hexagonal to the bcc structures at high temperatures (Zhang et al. 2005 and 2007) were inconsistent with previous study at temperatures around the room-T (Xia et al. 1991). Therefore, we reinvestigated the transformation pressure in zirconium metal.

The starting material used in this study was polycrystalline Zr. High-pressure X-ray diffraction experiments were carried out in an external heated diamond anvil cell. The small sample sandwiched between pellets of NaCl powder was loaded into a hole that had predrilled into a rhenium gasket. The heating temperature was up to 800 K, and was recorded using the R-type of thermocouples. The sample was probed using angle-dispersive X-ray diffraction, located on the synchrotron beam lines, at NE1A of the Photon Factory. Details of the synchrotron X-ray experiments have been described elsewhere (e.g., Ono et al. 2005). The angle-dispersive X-ray diffraction patterns were obtained on the imaging plate of an X-ray data collection system (Rigaku, RAXIS). The pressure was calculated from the NaCl unit cell volume using the equation of state (EOS) for NaCl, as developed by Ono (2010).

The boundary from the omega phase to the bcc phase was determined at high temperatures (300 - 800 K). Our results were in good agreement with those reported in previous room-temperature study. The gradient of dP/dT of the boundary was negative. However, the gradient observed in our experiments was 2-3 times more negative than that reported by previous high-temperature experiments (Zhang et al. 2005 and 2007). Our new data indicated that the difference in the stress conditions of the sample led to the discrepancy of the gradient of dP/dT slope in previous studies.

Keywords: Zirconium, Phase transition, High pressure and high temperature

Crystal structure analysis of a new high-pressure strontium silicate

SEKINE, Keisuke¹ ; ISHII, Takayuki¹ ; KOJITANI, Hiroshi^{1*} ; AKAOGI, Masaki¹

¹Dept. of Chemistry, Gakushuin University

SrSiO₃ is an analog material to CaSiO₃ which is an important component of the Earth's crust- and mantle-constituting minerals. High-pressure phase relation experiments in SrSiO₃ showed that δ'-SrSiO₃ is stable up to about 10 GPa and decomposes into BaGe₂O₅-III -type SrSi₂O₅ + larnite-type Sr₂SiO₄ between 14 and 20 GPa (Kojitani et al., 2005). Then, hexagonal perovskite-type SrSiO₃ becomes stable above about 20 GPa (Yusa et al., 2005). However, phases except for larnite-type Sr₂SiO₄ appearing in the pressure range between 10 and 14 GPa have been unclear. In this study, crystal structure and composition of one of the unknown phases were determined.

A sample for single-crystal structure analysis was synthesized by heating a mixture of pseudowollastonite-type CaSiO₃ and SiO₂ cristobalite (mole ratio of 1:1) with a little amount of water at 12 GPa and 1200 °C for 90 min using a Kawai-type multi-anvil high-pressure apparatus. A single-crystal sample with 120x80x60 μm was used for the single-crystal X-ray diffraction measurement. 953 reflection data were analyzed using the SHELX-97 software. Composition analysis of the high-pressure phase was performed using SEM-EDS.

The composition analysis showed that the new high-pressure phase had a composition of Sr₄Si₉O₂₂. The single-crystal structure analysis suggests the monoclinic crystal system with the space group of *C2/m*. Lattice parameters were determined to be $a = 13.3765(4) \text{ \AA}$, $b = 5.2321(2) \text{ \AA}$, $c = 11.6193(6) \text{ \AA}$, $\beta = 113.976(4) \text{ deg}$. *R* factor was 1.25%. The framework of the obtained crystal structure consists of two layers by corner-sharing single chains of edge-shared SiO₆ octahedra or SiO₅ rhombic pyramid polyhedra and by corner-shared SiO₄ tetrahedra and SiO₆ octahedra. It should be mentioned that this structure includes the SiO₅ rhombic pyramids which are very rare in silicates. Strontium ions in the structure are arranged between the two layers and are coordinated by seven oxygens. The structure of δ'-SrSiO₃ consists of four-membered rings of SiO₄ tetrahedra and strontium ions coordinated by seven oxygens. On the other hand, BaGe₂O₅-III type SrSi₂O₅ has a framework by corner-shared SiO₆ octahedra and SiO₄ octahedra and coordination number of Si²⁺ is 12. The crystal structure determined in this study is consistent with the fact that its density would be between those of the lower-pressure and higher-pressure phases.

Keywords: strontium silicate, high-pressure, single-crystal structure analysis, SiO₅ polyhedron

Heat capacity and entropy measurements by PPMS for high-pressure phases in TiO₂ and MnSiO₃

AKAOGI, Masaki^{1*} ; KOJIMA, Meiko¹ ; FUKAI, Aya¹ ; KOJITANI, Hiroshi¹

¹Dept. of Chemistry, Gakushuin University

Thermodynamic properties of high-pressure minerals are widely used to calculate phase relations at high pressures and high temperatures and to compare with the properties by the first-principles calculations. Standard entropy, $S_{298.15}$, is determined by integrating C_p/T in the temperature range between 0 and 298.15 K, where C_p is isobaric heat capacity and T is absolute temperature. To measure C_p at the temperature range, adiabatic calorimetry has been widely used with the highest precision. However, C_p of only a few high-pressure minerals have been measured so far, because a sample of more than several gram is required for the adiabatic calorimetry. Recently, low-temperature C_p measurement with thermal relaxation method using the Physical Properties Measurement System (PPMS) has been developed for samples of about ten milligram quantity. In this method, the sample is cooled with liquid helium and C_p is measured at about 2-310 K. By measuring the sample temperature change associated with applied heat pulse, thermal relaxation process is analyzed to obtain C_p . By this method, we measured C_p and determined $S_{298.15}$ for Mg₂SiO₄ wadsleyite and ringwoodite, MgSiO₃ akimotoite and perovskite, and SiO₂ stishovite, in collaboration with Atake-Kawaji laboratory, Tokyo Institute of Technology. Very recently, we have installed the PPMS apparatus in the laboratory in Gakushuin University, and have investigated C_p and S of rutile-type and α -PbO₂-type TiO₂ and garnet-type MnSiO₃.

Using a multianvil apparatus, rutile- and α -PbO₂-type TiO₂ phases were synthesized at 3 and 8 GPa, respectively, at 600-700 °C, and MnSiO₃ garnet was made at 15 GPa and 1000 °C. All the cylindrical samples were polished and fixed with grease on the stage in the PPMS. The C_p measurements in this study were performed at 2-308 K using the polycrystalline samples of 10-21 mg. The C_p measured for α -Al₂O₃ (NBS SRM-720) by the PPMS apparatus were consistent within experimental errors with those measured by adiabatic calorimetry by Ditmars et al. (1982).

The measured C_p of rutile-type TiO₂ were in good agreement with those by previous studies, and the obtained $S_{298.15}$ was 50.10 J/molK. Our C_p data of α -PbO₂-type TiO₂ were almost consistent with those with PPMS measurement by Yong et al. (2014), but substantially smaller than those with DSC measurement by Manon (2008). The $S_{298.15}$ of α -PbO₂-type TiO₂ was determined as 46.50 J/molK in this study. The C_p data of MnSiO₃ garnet indicated an anomaly at 15 K probably due to magnetic transition, and $S_{298.15}$ of 90.92 J/molK. High-pressure phase relations calculated using the above data are also reported.

Keywords: heat capacity, entropy, high-pressure phase, PPMS apparatus

Mechanisms of phase transitions of methane hydrate under high pressure

KADOBAYASHI, Hirokazu^{1*}; HIRAI, Hisako¹; HIRAO, Naohisa²; OHISHI, Yasuo²; OHTAKE, Michika³; YAMAMOTO, Yoshitaka³; KOJIMA, Yohei¹

¹Geodynamics Research Center, Ehime University, ²Japan Association of Synchrotron Radiation Institute, ³National Institute of Advanced Industrial Science and Technology

Methane hydrate (MH), called as “ burning ice ”, is expected to be a fruitful natural resource, at the same time, methane is rather effective greenhouse gas than carbon dioxide. It is also thought to be a major constituent of icy bodies in and outside the solar system. MH is composed of hydrogen-bonded host water molecules forming cages or frameworks that include guest methane molecules. Three phases of MH have been known so far. The low-pressure phase, sI, is stable below 0.8 GPa and it transforms into a hexagonal structure, sH, at 0.8 GPa and further transforms to a filled ice Ih (FIIhS) at 1.8 GPa at room temperature. At these phase transitions, release of water content is accompanied. As described above, the existence of phase transitions and the structures of transformed high-pressure phases have been clarified by the previous studies. However, transition mechanisms from the lower-pressure phase to individual high-pressure phases have been unresolved issue. In this study, high-pressure experiments were performed to investigate mechanisms of the phase transitions of MH at high pressures.

Clamp type and lever-spring type diamond anvil cells were used in this study. The pressure and temperature conditions were from 0.2 to 3.0 GPa and 300 K, respectively. Pressure measurements were made via a ruby fluorescence method. The initial samples of MH were prepared by ice-gas interface method. The samples were characterized via time-resolved X-ray diffractometry using synchrotron radiation at BL-10XU, SPring-8, and time-resolved Raman spectroscopy at GRC, Ehime University.

As for sI-sH phase transition, Raman spectroscopy revealed that 5^{12} cages of sI survived during the transition and that the 5^{12} cages remained as same 5^{12} cages of sH structure. And, $5^{12}6^2$ cages of sI changed to $4^35^66^3$ and $5^{12}6^8$ cages of sH. The results suggested that the sI-sH transition may follow a martensitic-like mechanism because of being maintaining 5^{12} cages unchanged in sH structure. On the other hand, at sH-FIIhS transitions, Raman spectroscopy detected abrupt collapse of all constituent cages in sH and release of fluid or solid methane molecules. And then, the framework of FIIhS was gradually reconstructed, absorbing the released methane molecules into the FIIhS structure. The results indicated that the sH-FIIhS transition follows reconstructive mechanism. The explanations may be reasonable, because the former transition is from a cage to another cage structure, and the latter one is from a cage structure to different framework of a filled ice structure.

Keywords: methane hydrate, mechanisms of phase transitions, high-pressure, X-ray diffractometry, Raman spectroscopy

Incorporation of NaCl into ice VI and ice VII under high pressure.

HIRAI, Hisako^{1*} ; YAMASHITA, Fukunori¹ ; KAGAWA, Shingo¹ ; KADOBAYASHI, Hirokazu¹ ; OHISHI, Yasuo² ; YAMAMOTO, Yoshitaka³

¹Geodynamics Research Center, Ehime University, ²JASRI, ³AIST

Icy satellites have been thought to contain a large amount of salts besides water ices. Ice exhibits a wide variety of forms consisting of hydrogen-bonded water molecules. More than sixteen stable and metastable forms have been reported so far. Liquid water can dissolve various kinds of solutes. Whereas, in the previous idea, when water crystallizes, the dissolved solutes are excluded, which results in formation of pure water ices. Recently, Frank et al. [1] and Komatsu et al. [2] reported that NaCl or other salts was incorporated into ice VI and/or ice VII. In these studies, however, it has been still unclear which ice can incorporate NaCl, and amount of salts incorporated and states of the salt in the ice structure have not yet been clarified. In this study, in order to understand possible incorporation of salts in to ice VI and VII structures, high-pressure experiments were performed with a system of H₂O-NaCl, a typical salt, at room temperature.

Lever-and-spring type diamond anvil cell was used. Pressure range examined was from 0.2 to 10 GPa. NaCl aqueous solutions with three concentrations, 1.5, 2.5, and 5.0 w%, were prepared as starting samples. Characterization was made by optical microscopy, X-ray diffractometry (XRD), and Raman spectroscopy.

Similar phase changes were observed for the samples with three different concentrations. The NaCl aqueous solutions finally crystallized to form ice VI above 1.6 GPa, although in case of pure water ice VI is formed at 1.0 GPa at room temperature. At the pressure range from 2.1 to 3.2 GPa, a new high-pressure phase, of which diffraction pattern was not explained by ice VI, ice VII, and solid NaCl, was observed. Above 3.2 GPa, ice VII and solid NaCl appeared. The high-pressure phase observed may correspond to a phase having a modified structure of NaCl-dihydrate reported by Nakayama et al. [3]. Unit cell volumes of ice VII calculated expanded larger than those of pure ice VII. The result was opposite sense to those by Frank et al, where the volumes decreased smaller than those of pure ice VII. The amounts of the volume expansion for 2.5 and 5.0 w% samples were larger than those of 1.5 w% samples. The volume expansions of the former two samples were almost similar. The results suggested that limitation of incorporation into ice VII is less than 2.5 w%. The O-H vibrational modes shifted to higher frequencies by 10 to 20 cm⁻¹ and 5 to 10 cm⁻¹ from those of pure ices for ice VI and ice VII, respectively.

All experimental results indicated that NaCl is incorporated both into ice VI and ice VII at room temperature. The amounts of incorporation were estimated to be up to 2.5 w%. Such large amount of incorporation of salt is expected to effect on physical properties of ices, which is important in inferring the interiors of icy bodies.

1. M. R. Frank et al., PEPI 155 (2006) 152; M. R. Frank et al., PEPI 170 (2008) 107; M. R. Frank et al., PEPI 215 (2013) 12.
2. K. Komatsu et al., Abstract of Annual meeting of Jpn. Society High Pressure Tech. (2010).
3. K. Nakayama master thesis (2012).

Keywords: high-pressure ice, NaCl, incorporation, icy satellite

Structure refinement of legrandite and paradamite : crystal chemistry and hydrogen bonds

JINNOUCHI, Satoshi^{1*} ; YOSHIASA, Akira¹ ; SUGIYAMA, Kazumasa² ; ARIMA, Hiroshi² ; SHIMURA, Reiko² ; MIYAWAKI, Riturou³

¹Graduate School of Science and Technology, Kumamoto University., ²Institute for Materials Research, Tohoku University,
³National Science Museum

Legrandite, $Zn_2AsO_4(OH)H_2O$ and paradamite, $Zn_2AsO_4(OH)$, are zinc arsenate minerals and have a color between pale yellow and yellowish brown. Related minerals of legrandite and paradamite are adamite, $Zn_2AsO_4(OH)$, and so on with different structures. We performed the structure refinement of legrandite and paradamite Oujela Mine, Mapimi, Durango, Mexico, by (RAPID) RIGAKU single-crystal structure analysis system. We determined the hydrogen position by difference Fourier method. We revealed the detail hydrogen bond using bond valence calculation and hydrogen positions and compared crystal structures of these. The structure of legrandite is constituted by two AsO_4 tetrahedrons, ZnO_6 octahedron and three ZnO_5 trigonal dipyramids that have large unique distortion. AsO_4 tetrahedron, ZnO_5 trigonal dipyramid and ZnO_6 octahedron constitutes the unique framework. The structure of paradamite is constituted by AsO_4 tetrahedron and two ZnO_5 trigonal dipyramid that have large unique distortion. In legrandite, 5 coordination of trigonal dipyramids have a distance to be expected from ionic radii but interatomic distance of Zn(3)-O(1) has extraordinary distance. Two OH groups bond to Zn1 and Zn2, Zn3 and Zn4 make the $ZnO_3(H_2O)_2$ trigonal dipyramid that is bonded to two H_2O group in legrandite. In paradamite, Zn1 and Zn2 make $ZnO_3(OH)_2$ and $ZnO_4(OH)$ trigonal dipyramid. Hydrogen atoms make a lot of hydrogen bonding in legrandite and paradamite. Crystal structure of legrandite has a tunnel structure continuous that is only parallel to c axis and similar structure is observed in paradamite only parallel to a axis. There are path of proton-conduction in these direction and we conjecture that these proton-conductivity have large anisotropy of one dimension.

Keywords: structure refinement, legrandite, paradamite, crystal chemistry, hydrogen bonds

Structure analysis of deuterated brucite at pressures to 3 GPa by pulsed neutron powder diffraction

OKUCHI, Takuo^{1*} ; TOMIOKA, Naotaka¹ ; PUREVJAV, Narangoo¹ ; HARJO, Stefanus² ; ABE, Jun³ ; WU, Gong²

¹Institute for Study of the Earth's Interior, Okayama University, ²Japan Atomic Energy Agency, ³CROSS Tokai

Atomic-scale structures around hydrogen atoms in hydrous minerals may significantly change with increasing pressure, which affect thermodynamic stability, optical properties (Raman, IR, etc.), and transport phenomena of the relevant minerals. To directly observe such structure change around hydrogen atoms, we have conducted neutron diffraction experiments of deuterated brucite at high pressures to 2.8 GPa, using a high-resolution neutron powder diffractometer recently installed at J-PARC Materials and Life Science Experimental Facility. To discriminate subtle structure change of deuterium site positions with increasing pressure, the quality of observed diffraction patterns has been considerably improved from the corresponding previous studies by adopting a new-type experimental apparatus and facility. A newly-designed opposed anvil cell apparatus optimized for the pulsed neutron beam (Okuchi et al., *High Pressure Research*, 33, 777, 2013) was effectively coupled with the time of flight diffractometer TAKUMI, which was designed to have the resolution of $\Delta d / d \sim 0.3\%$ along with moderately-intense beam and low background (Harjo et al., *Materials Science Forum*, 524, 199). We used single crystal diamond anvils with culet diameter of 2 mm for sample compression along with deuterated glycerine pressure medium. The combination gives very high neutron transparency as well as high resolution to enable accurate structure refinements of tiny sample volume of the order of less than 1 mm³. Through Rietveld refinements of the observed patterns, tilting of all OD dipoles in the compressed brucite toward one the three nearest-neighbor oxygen anions in the brucite structure was confirmed to be substantial at the observed pressure regime, suggesting the formation of pressure-induced hydrogen bonding. Therefore, at lower crust and mantle wedge conditions, this pressure-induced bonding may play an important role to constrain hydrogen into the relevant hydrous minerals.

Keywords: hydrogen, brucite, high pressure, neutron diffraction

Factors controlling barite-water distribution of selenium oxyanion

TOKUNAGA, Kouhei^{1*}; YOKOYAMA, Yuka¹; TAKAHASHI, Yoshio¹

¹Department of Earth and Planetary Systems Science, Graduated School of Science, Hiroshima University

Geochemical behavior of trace elements is controlled by their interaction with major minerals through ion exchange, sorption/desorption, and coprecipitation/dissolution processes, which govern the concentrations of trace elements in natural water. Especially, the coprecipitation process with mineral is potentially important because trace elements can be incorporated and immobilized in the crystal lattice at least until the minerals are dissolved. Previous studies showed that the partitioning behaviors of trace elements to minerals were controlled by many complex factors, such as crystal constraints of ion substitution, effects of complexation in the aqueous phase, rate of crystallization, and changes in temperature or pressure. For instance, Yokoyama [2011, 2012] demonstrated that, in the case of arsenic (As) and selenium (Se) incorporation into calcite, arsenate rather than arsenite is selectively incorporated into calcite, whereas selenite (Se(IV)) rather than selenate (Se(VI)) into calcite because of the high stabilities of calcium arsenate and calcium selenate complexes compared with those for arsenite and selenite. In this study, we focused on the distribution behavior of Se into barite to determine the factors controlling the partitioning behaviors of the trace elements to minerals at the molecular scale by X-ray absorption fine structure (XAFS). Our previous results suggested that the distribution behavior of Se into barite was controlled by two factors: the stability of the surface complex between barite and Se species (=chemical affinity) at the initial process and the stability of the ion substitution in the crystal structure (=structural affinity) for the subsequent process. In this presentation, the barite-water distributions of Se controlled by the structural affinity are highlighted.

The coprecipitation experiments were conducted to examine the influence of ion substitution structure on the distribution behavior of Se into barite as a function of the reaction time in term of the variation of barite morphology, total concentration, oxidation states, and coordination structure of Se in barite. The results showed that both total Se concentration and the Se(VI)/Se(IV) ratio in barite increased abruptly within first 24 hour and almost reached equilibrium after 24 hours. EXAFS analysis for the initial and aged samples showed that the coordination number of Se-Ba in the aged sample is larger than that in the initial stage. The results indicates that a larger amount of Se(VI) than Se(IV) was incorporated from adsorption site on the surface into the barite crystal by substituting sulfate site because of their high crystallinity that can excludes Se(IV) to a larger degree than Se(VI) due to the similar structure of sulfate ion and sulfate. Based on these results, it is considered that the Se(VI) was preferentially incorporated into barite due to its high structural affinity than Se(IV), thus, the Se(VI)/Se(IV) ratios in barite relatively increased through crystallization. These results suggest that structural affinity is an important factor for controlling the distribution behavior of Se between barite and water.

Keywords: barite, selenite, selenate, XAFS, distribution behavior, structural affinity

Mid- and far-infrared spectroscopy for Li-Al-Mg micas

MAKIO, Masato^{1*} ; ISHIDA, Kiyotaka¹

¹Graduate School of Social and Cultural Studies

Mica is a one of the major rock forming minerals and widely spread in the earth crust. The hydrothermal synthetic Li-Al-Mg trioctahedral mica series were measured by mid- and far-infrared spectroscopy and X-ray powder diffraction Rietveld refinement: (a)Trilithionite: $K(Li_{1.5}Al_{1.5})(AlSi_3)O_{10}F_2$ - Phlogopite: $KMg_3(AlSi_3)O_{10}F_2$, (b)Polyolithionite: $K(Li_2Al)Si_4O_{10}F_2$ - Tainiolite: $K(LiMg_2)Si_4O_{10}F_2$, (c)Polyolithionite- Eastonite: $K(Mg_2Al)(Al_2Si_2)O_{10}F_2$ and OD- FMg- Masutomilite: $K(LiAlMg)AlSi_3O_{10}(F, OD)_2$.

The Li-Al-Mg micas synthesized hydrothermally at 600- 650 °C and 150- 200MPa in cold-seal externally heated Tuttle-type vessels. The starting materials were mixed and then sealed in Pt/Au capsules with 20 wt % D₂O (99.9 % in purity). X-ray Rietveld analysis was done using Rietan- 2000 (Izumi and Ikeda 2000). Mid- and far-infrared spectra were measured with JASCO FTIR- 620 spectrometer. Each sample was scanned 256 times in an evacuated sample-chamber.

All samples could refine monoclinic, C2/m (1M polytype). In the 250- 50cm⁻¹ far-infrared region, three kinds of bands are observed: these bands due to an in- plane tetrahedral torsional band between 170- 150cm⁻¹, an interlayer K- O_{inner} stretching band between 120- 140 cm⁻¹ and K- O_{outer} stretching band between 90- 100 cm⁻¹. With increasing <K- O_{inner}>, K- O_{inner} stretching band shifts higher frequency, while with increasing <K- O_{outer}>, K- O_{outer} stretching band shifts lower frequency. In the 650- 250cm⁻¹ mid- and far-infrared region, two parts of bands are observed. With increasing ^[4]Si→Al, (Si,Al)- O deformational band in the range of 600- 400cm⁻¹ became broad and merged.

Keywords: Li-Al-Mg mica, hydrothermal synthesis, mid-infrared, far-infrared, Rietveld analysis

Cesium (Cs) Sorption Experiments into Weathered Biotite in Fukushima

KIKUCHI, Ryosuke^{1*} ; KOGURE, Toshihiro¹

¹Earth and Planetary Sci., Univ. Tokyo

After the accident of Fukushima Daiichi nuclear power plant in March 2011, radioactive contamination of the soil around the plant has become an urgent problem in Japan. Previous studies proposed that weathered micaceous minerals present favorable sorption environments for Cs⁺. Because the contaminated areas in Fukushima are mainly covered with weathered granite soil, weathered biotite with hydrated (vermiculite) interlayers is abundant. Hence basic understanding of Cs⁺ sorption process into the biotite is important to find the recipe for decontamination of radiation. Some of previous studies reported that Cs⁺ is adsorbed mainly at the frayed-edge sites of such micaceous crystals. However, other studies indicated that Cs⁺ penetrates deeply inside the crystals, along the interlayer regions by ion-exchange. In this study, we performed Cs⁺ sorption experiments using single-crystals of Fukushima weathered biotite with well-regulated edge surfaces, and considered the relationship between the weathering state of biotite and Cs⁺ sorption property.

Fresh and two kinds of weathered biotite were collected from granodiolite of Abukuma granite body in Fukushima prefecture. For each sample, cross sections of <1 mm thick perpendicular to the basal planes were prepared. Surface damage formed by the mechanical grinding/polishing was removed by Ar⁺ ion sputtering. These sections were immersed in 30 mL of CsCl aqueous solution of 2000 / 200 / 20 / 0 ppm for 24 hours at room temperature to incorporate Cs⁺.

After the reaction, the surfaces of the sections were investigated using scanning electron microscopy (SEM) with energy dispersive X-ray spectroscopy (EDS). SEM-EDS with various acceleration voltage indicated that the concentration of the sorbed Cs⁺ does not change in the depth direction of ~several microns range. Cs⁺ was apparently sorbed at 2000 ppm but not at 200 ppm for fresh biotite, whereas Cs⁺ was sorbed at both concentrations in the weathered biotite. Back-scattered electron (BSE) images and EDS analysis showed preferred sorption of Cs⁺ at the regions probably with dense vermiculite interlayers in the weathered biotite. Moreover, some specimens were processed into thin foils using focused ion beam (FIB) and examined using scanning transmission electron microscopy (STEM). High-angle annular dark field (HAADF) imaging in STEM has visualized Cs⁺-incorporated interlayer regions individually in the weathered biotite.

Keywords: Biotite, Vermiculite, Cesium, SEM-EDS, FIB, HAADF-STEM

Pressure-induced phase transitions of vaterite, a metastable phase of calcium carbonate

MARUYAMA, Koji^{1*}; KOMATSU, Kazuki¹; KAGI, Hiroyuki¹; YOSHINO, Toru²; NAKANO, Satoshi³

¹Geochemical Research Center, Univ. Tokyo, ²TIRI, ³National Institute for Materials Science

1. Introduction

Calcium carbonate is one of the most common and ubiquitous minerals on the Earth's surface and plays an important role in global carbon cycle. There are many studies about high-pressure behavior of calcite and aragonite. At ambient temperature, calcite transforms to calcite II at about 1.5 GPa and to calcite III at about 2.0 GPa. The transition from aragonite to post-aragonite phase was observed at about 40 GPa. In contrast, no study has been reported on the high-pressure behavior of vaterite, which is a metastable phase of CaCO₃, and is known as a precursor material of more stable CaCO₃ polymorphs, calcite and aragonite. In this study, the high-pressure behavior of vaterite was investigated by in situ synchrotron X-ray diffraction (XRD) experiments using a diamond anvil cell.

2. Experimental method

In this study, vaterite was synthesized by mixing two aqueous solutions, 60 mM CaCl₂ aq. and 60 mM NaHCO₃ aq., kept at 30 degree C. The mixed solution was sealed in a plastic bottle and stirred for 10 min at 30 degree C, and then filtered using an aspirator, washed by pure water, and dried at about 130oC. The obtained white powder was identified as pure vaterite using powder XRD method.

High-pressure experiments were carried out using a diamond anvil cell (DAC). The synthesized vaterite and several tiny ruby crystals were loaded into a gasket hole together with helium as a pressure transmitting medium. The pressure was changed between 0-14 GPa, which was measured by the ruby fluorescence method. XRD patterns were measured at each pressure at room temperature. X-ray diffraction observations were carried out at room temperature using the synchrotron beam line of BL18C in the Photon Factory, Japan.

3. Results and discussion

XRD patterns recorded at pressures lower than 4.7 GPa indicated that the sample consists of vaterite only. At 4.7 GPa, main three peaks of vaterite were split and a peak assignable to calcite III appeared. The discontinuous changes in axial lengths were observed by refinement of lattice constants using a crystal structure model proposed by Le Bail et al. (2011). This change suggests a pressure-induced phase transition from vaterite to a high-pressure form (hereafter vaterite II). Change in the diffraction intensities suggested that vaterite II transformed to calcite III with increasing pressure up to about 9 GPa. At 12.9 GPa, new diffraction spots were observed. These spots were not explainable with the diffraction peaks from any polymorphs of CaCO₃. This implies that the new spots are derived from another high-pressure phase of vaterite (vaterite III). After decompression, the recovered sample was identified as a mixture of calcite and vaterite. These results indicate that the transition from vaterite II to calcite III is irreversible. In this study, new high-pressure phases of CaCO₃ (vaterite II and III) were discovered by high-pressure experiments of vaterite at ambient temperature.

Keywords: vaterite, phase transition, high-pressure

Huge plastic deformation of SiO₂ glass at room temperature

WAKABAYASHI, Daisuke^{1*} ; FUNAMORI, Nobumasa¹ ; SATO, Tomoko²

¹Department of Earth and Planetary Science, University of Tokyo, ²Department of Earth and Planetary Systems Science, Hiroshima University

Covalent solids are known to be hard but brittle. Moreover, glasses do not deform plastically by dislocation movement seen in crystals due to the lack of long-range order. However, SiO₂ glass, a highly covalent glass, has long been known to be densified up to about 20% by applying high pressure. This phenomenon is called permanent densification, which is some kind of phase transformation caused by the reconstruction of the network structure consisting of SiO₄ tetrahedra [e.g., Wakabayashi et al., 2011], and could be considered as plastic deformation in a broad sense. Recently, the differential strain of SiO₂ glass in its intermediate-range structure, corresponding to the first sharp diffraction peak, was measured under uniaxial compression by a radial X-ray diffraction method, in which X-rays irradiate the sample from a direction perpendicular to the compression axis (i.e., from a radial direction) [Sato et al., 2013]. In those measurements, very large differential strains were observed under pressure and surprisingly also after decompression. This residual strain may be attributable to the anisotropic reconstruction of the network structure (i.e., anisotropic permanent densification).

In this study, the change in size of bulk samples was measured for uniaxially-compressed SiO₂ glass to clarify whether SiO₂ glass undergoes plastic deformation in a narrow sense, i.e., without density change. X-ray diffraction measurements were also conducted in a wide Q-range with 50 keV monochromatic X-rays by irradiating the recovered sample from the radial direction to clarify whether a differential strain remains only in the intermediate-range network structure or also in the short-range SiO₄ tetrahedral structure. Pressures were generated by using a diamond-anvil cell. The starting material was in the form of a disk, and was adjusted to have an appropriate initial thickness to be compressed under uniaxial conditions, i.e., pinched directly by the two anvils, above a certain pressure. Three independent experiments were conducted with an argon pressure medium up to 20 GPa in run 1, 12 GPa in run 2, and 6 GPa in run 3. The change in size of sample was measured with an optical microscope. X-ray diffraction measurements were carried out at PF AR-NE1. All the experiments were conducted at room temperature.

In runs 1 and 2, the diameter of sample was found to increase significantly with pressure from 6-8 GPa, where uniaxial conditions were achieved, to the maximum pressure of each run without fracturing, and it became about 15% larger at 20 GPa than at 0 GPa. The macroscopic differential strain was about an order of magnitude larger than the microscopic differential strain reported in the previous study [Sato et al., 2013], suggesting that SiO₂ glass deformed plastically at room temperature. The X-ray diffraction measurements clarified that the recovered samples were in the fully densified state (about 20% densified). It was also revealed that a residual differential strain was observed only in the intermediate-range network structure and its magnitude was consistent with the previous study [Sato et al., 2013]. On the other hand, in run 3, the sample did not deform plastically by uniaxial compression from 2-3 GPa to 6 GPa. The X-ray diffraction pattern of the recovered sample was the same as that of the ordinary SiO₂ glass. Permanent densification is known to begin at about 9 GPa under hydrostatic conditions [e.g., Wakabayashi et al., 2011], and it is suggested that permanently densified SiO₂ glass easily undergoes plastic deformation even at room temperature.

D. Wakabayashi et al., *Phys. Rev. B* **84**, 144103 (2011).

T. Sato et al., *J. Appl. Phys.* **114**, 103509 (2013).

Keywords: SiO₂ glass, plastic deformation, permanent densification, network structure

Shock compression of synthetic amino acid - silica gel complex modeling for comet nucleus

MURAI, Takuro¹ ; OKUNO, Masayuki^{2*} ; OKUDERA, Hiroki² ; ARASUNA, Akane¹ ; MASHIMO, Tsutomu³ ; CHEN, Liliang³ ; MIZUKAMI, Tomoyuki² ; ARAI, Shoji²

¹Graduate School of Kanazawa University, ²Kanazawa University, ³Kumamoto University

Some amino acids were found in comet coma particle and Murchison meteorite [1,2]. These reports may suggest a possibility that basic materials of primitive life on the earth were formed in the space and delivered to the earth.

Greenberg et al. (1997)[3] reported the almost comets are made of organic compounds, silicates and ice. On the other hand, silica gel contains a non crystalline $\text{SiO}_{4-n}(\text{OH})_n$ framework with water molecules. So, silica gel is a suitable model material for comet. In this study, in order to investigate the stability of amino acid (L-serine) in the comet nucleus during the impact to the earth, synthetic amino L-serine - silica gel complex materials were shock compressed and the structure change of the recovered samples were analyzed by X-ray diffraction measurements, IR and Raman spectroscopies. Shock compression experiments were performed at 8.2, 10.9, 19.7 and 26.9 GPa.

By Raman spectroscopic analyses, it was indicated that synthetic complex materials include two types of L-serine such as crystalline L-serine and hydrated L-serine. Obtained Raman spectra of shocked materials show the L-serine crystal was disappeared and hydrated L-serine molecules survived at 19.7 GPa of shock pressure. Therefore, the sample at 19.7 GPa includes only hydrated L-serine molecules. This may indicate that intermolecular hydrogen bonds of L-serine molecules may be broken by shock compression with water molecule.

The shock pressure of 19.7 GPa is consistent with the estimated impact pressure of about 19% comets to the earth reported by Blank et al. (1999) [4]. This fact may indicate that a possibility for the basic materials of primitive life on the earth were formed in the space and delivered to the earth.

References

- [1] Elisila J.E., Glavin D.P., Dworkin J.P. (2009) Cometary glycine in samples returned by stardust. *Meteoritics & Planetary Science* 44, 1323-1330
- [2] Cronin J.R. and Pizzarello S. (1983) Amino acid in meteorites. *Advances in space research* 3, 5-18
- [3] Greenberg J.M., Aigen Li (1997) Silicate core-organic refractory mantle articles as interstellar dust and as aggregates in comets and stellar disks. *Advance in space research* 19, 981-990
- [4] Blank J.G., Millar G.H., Michael J.A., Winas R.E. (1999) Experimental shock chemistry of aqueous amino acid solution and cometary delivery of periodic compounds. *Origin of Life and Evolution of the Biosphere* 31, 15-51

Keywords: comet, amino acid, silica gel, shock compression

Microtexture and formation mechanism of impact diamonds from the Popigai crater, Russia

OHFUJI, Hiroaki^{1*} ; YAMASHITA, Tomoharu¹ ; LITASOV, Konstantin² ; AFANASIEV, Valentin² ; POKHILENKO, Nikolai²

¹Geodynamics Research Center, Ehime University, ²Siberian Branch of the Russian Academy of Sciences

Large meteoritic impact occasionally produces an extensive amount of diamond on the surface of the Earth [1, 2]. Popigai crater located in the north central Siberia is a typical example of such diamond-forming shock events and has recently been brought back into the spotlight due to its vast estimated reserves of the impact diamonds [2-4]. Authigenic impact diamonds occur in shocked graphite-bearing garnet-biotite gneisses that are found as inclusions in impact melt rocks, so-called tagamites and suevites. Popigai diamonds occur as irregular to tabular grains of 0.5-2 mm size (up to 10 mm) and usually show yellow, gray or black colors [3]. Electron microscopic (SEM and TEM) observations in previous studies described that they are polycrystalline aggregates of 0.1-1 μm grains and show a distinct preferred orientation along the [111], which is in a coaxial relation to the [001] of the original graphite source [2-4]. This crystallographic feature as well as the occasional coexistence of lonsdaleite, a metastable carbon polymorph, suggest the Martensitic phase transformation for the potential formation process of the impact diamonds from Popigai crater. However, the textural feature of the impact diamonds and its variation has not fully been examined. Here, we present the result of detailed microtextural observations of impact diamonds from the Popigai crater by transmission electron microscopy (TEM) and discuss the formation mechanism and condition in comparison with those of synthetic diamonds obtained by high pressure and high temperature experiments.

In total 10 diamond grains (7 transparent yellowish and 3 black samples) from the Popigai crater were studied. Each sample was first analyzed by a micro-focus XRD equipped with a Mo target and an IP detector. The results showed that transparent samples consist mostly of diamond and occasionally contain lonsdaleite, while black ones are a mixture of graphite, lonsdaleite and diamond, which are all in a coaxial relation as shown by 2D diffraction patterns collected in transmission geometry. Each sample was then transferred to a focused ion beam (FIB) system to cut out TEM foil sections perpendicular to the surface (of the tabular grains). TEM observation revealed that although all the samples commonly possess layered structures and preferred orientation (mostly along [111] of diamond), there are varieties in crystallite (grain) size (down to 10-20 nm) and degree of preferred orientation. Taking into account the similarity in texture and preferred orientation feature between the Popigai diamonds and synthetic diamond, the variation is likely derived from the small difference in crystallinity of the starting graphite sources and perhaps more significantly from the difference in shock temperature.

According to the shock features recorded in the silicate minerals of the diamond-bearing impactites, the threshold pressure for the onset of the graphite-diamond transformation is estimated to be 34-36 GPa [3]. However, our recent experimental synthesis [5] demonstrated that a similar phase assembly (mostly diamond + traces of lonsdaleite) and microtexture can be produced at much lower pressures of 15-25 GPa at >2000 °C. The shock pressure as well as shock- and post-shock temperature accompanied with the formation of the Popigai crater might be needed to be reevaluated carefully to understand the real nature of the giant impact.

- [1] Masaitis V.L. (1998) *Meteoritics & Planetary Science*. 33. 349-359.
- [2] Langenhorst F., Shafranovsky G.I., et al. (1999) *Geology*. 27. 747-750.
- [3] Deutsch A., Masaitis V.L., et al. (2000) *Episodes*. 23. 3-11.
- [4] Koeberl C., Masaitis V.L., et al. (1997) *Geology*. 25. 967-970.
- [5] Isobe F., Ohfujii H., et al. (2013) *Journal of Nanomaterials*. 2013. 380165.

Melting and crystal growth textures developed in rapid heating and cooling of olivine fine particles

ISOBE, Hiroshi^{1*} ; GONDO, Takaaki¹

¹Grad. Sch. Sci. Tech., Kumamoto Univ.

Olivine is one of the most common mineral in the solid Earth and chondritic meteorites. Olivine crystals show characteristic textures in chondrules depending on heating and cooling histories in chondrule formation processes at the early solar system. In this study, quick heating and cooling experiments of mixed olivine particles were carried out with a fine particles free falling apparatus (Isobe and Gondo, 2013). In the run products, characteristic melting and crystal growth textures controlled by phase relations, diffusion, and nucleation and growth behavior of olivine can be seen.

Starting material is mixed powder of natural olivine (Fo90), fayalite and an artificial olivine (Fo55). The typical diameter of the starting material particles is approximately 100 micron meters. Each particle is single crystal of olivine or mixture of two or three kinds of raw materials. Heating and cooling experiments are carried out in a high temperature furnace with mass flow controllers to regulate oxygen fugacity and total gas flow rate. Particles can be heated to 1400 degrees C within two seconds, are kept over 1400 degrees C approximately one second and quenched within a second. Maximum temperature has negative correlation to diameter of the particles, and cooling rate has positive correlation to the diameter depending on the falling velocity of the particles. Run products show spherical shape when the particles mostly melted, and are crystal fragments when the particles did not melt. The outside shape of the retrieved run products are observed with a scanning electron microscope. Inner textures of the particles are observed on polished section of the particles. Chemical compositions are also analyzed on the sections.

Fayalite grains are completely melted and Fo90 olivine grains are not melted by themselves concordantly with the phase relation of olivine. Internal textures of Fo55 olivine crystals show quick partial melting when the temperature reach solidus temperature. In the mixed olivine particles, relict crystals of Fo90 and Fo55 olivines dissolve to iron-rich melt derived from melting of fayalite. The dissolution of relict crystals produce steep chemical gradient at interface between crystals and melt.

Run products like barred olivine chondrules or melted cosmic spherules are produced from completely melted particles. In the particles including relict crystals, overgrowth textures from the relict crystals can be seen. Dendritic olivine crystals with regulated crystallographic orientation are developed in melted particles. Surface texture of melted particles may be affected by the dendritic olivine crystals. Oriented magnetite dendrites may also occur between olivine crystals when oxygen fugacity was in the magnetite stability field. Melting, nucleation and crystal growth processes in a few seconds can be discussed from the textures in the run products.

Keywords: Olivine, chondrule, nucleation, crystal growth, dendrites, quench texture

Temperature-dependent thermal expansivities of aluminum-free silicate melts and borosilicate melts

SUGAWARA, Toru^{1*}; KATSUKI, Junki²; YOSHIDA, Satoshi²; MATSUOKA, Jun²; MINAMI, Kazuhiro³; OCHI, Eiji³

¹Akita University, ²The University of Shiga Prefecture, ³Japan Nuclear Fuel Limited

Thermal expansivities (dV/dT) of silicate melts are essential in a thermodynamic calculation of phase equilibria in magmatic system as a function of pressure and temperature and in a numerical simulation of flow and thermal structures in glass melting furnace. Previous studies have been suggested that the dV/dT of aluminosilicate melts (Lange, 1996; Potuzak et al., 2006) and magmatic silicate melts (Lange, 1997; Ghiorso and Kress, 2004) is a function of composition, but independent of temperature. On the other hand, it has been reported that the dV/dT of $\text{SiO}_2\text{-TiO}_2\text{-Na}_2\text{O}$ melt (Liu and Lange, 2001) and $50\text{SiO}_2\text{-25CaO-25MgO}$ melt (Gottsmann and Dingwell, 2000) decrease with increasing temperature. Recently, we found that simulated-radioactive waste glass melt which has sodium-borosilicate composition also shows negative temperature-dependent dV/dT (Sugawara et al., 2013). We carried out density measurements for sodium-silicate melts ($(100-x)\text{SiO}_2\text{-xNa}_2\text{O}$, $x=23$ or 32.3 mol%), commercial soda-lime silicate melt ($71\text{SiO}_2\text{-6MgO-9CaO-14Na}_2\text{O}$, mol%) and borosilicate melts ($66.6\text{SiO}_2\text{-yB}_2\text{O}_3\text{-(33.33-y)Na}_2\text{O}$ where $y=8.3, 16.6, 25$; $66.6\text{SiO}_2\text{-(12.5+z)B}_2\text{O}_3\text{-(4.2-z)Al}_2\text{O}_3\text{-zCaO-(16.7-z)Na}_2\text{O}$ where $z=0$ or 4.2 mol%). The temperature and compositional dependences of the dV/dT are discussed based on the new density data and the literature data.

The high-temperature density (dHT) measurement has been made by double-bob Archimedean method between 1173K and 1665K. The glass samples were annealed around glass transition temperature (T_g) for 6-396 hours and quenched. Then the density of annealed glasses at 298K (d298) and linear thermal expansivity (dL/L) were determined by Archimedean method and TMA, respectively. The densities of supercooled melt around T_g (dTg) were calculated from the d298 and the dL/L of glasses. Then, molar volume as a function of temperature and the dV/dT of melts were obtained by combining the dTg and the dHT.

The dV/dT values of all samples examined in this study show negative temperature dependence. In the sodium silicate melts, the temperature dependence of the dV/dT is remarkable when the SiO_2 content increases from 50 to 67 mol%, while the dV/dT becomes close to zero as further increase in the SiO_2 content. The negative temperature-dependent dV/dT observed in the $71\text{SiO}_2\text{-6MgO-9CaO-14Na}_2\text{O}$ melt can be reproduced by an additive sum of the dV/dT of $67.8\text{SiO}_2\text{-32.2Na}_2\text{O}$, diopside (Gottsmann and Dingwell, 2000) and wollastonite (Potuzak et al., 2006) melts. High-temperature Raman spectroscopy for the $\text{SiO}_2\text{-Na}_2\text{O}$ and $\text{SiO}_2\text{-Na}_2\text{O-MgO}$ melts has been indicated that amount of Q4 species increases with increasing temperature and SiO_2 and MgO contents (Maehara et al., 2004, 2005). Therefore, the temperature dependent dV/dT for the sodium-silicate, commercial soda-lime silicate and diopside melts can be rationalized by an increase of rigid Q4 species at high temperature. The temperature dependence of the dV/dT is most remarkable in the $66.6\text{SiO}_2\text{-8.3B}_2\text{O}_3\text{-25Na}_2\text{O}$ melt among the borosilicate melts. The dV/dT decreases with replacement of Na_2O by B_2O_3 or CaO and of B_2O_3 by Al_2O_3 , suggesting that partial molar dV/dT of B_2O_3 depends on temperature-induced coordination change of boron and their composition dependence (Wu and Stebbins, 2010).

Acknowledgements: This work was a part of the research supported by Japan Nuclear Fuel Limited with Grant-in-Aid by the Ministry of Economy, Trade and Industry.

Keywords: silicate melt, thermal expansivity, densitometry